IEEE Access
Multidisciplinary | Rapid Review | Open Access Journal

Received October 29, 2018, accepted November 14, 2018, date of publication December 10, 2018,
date of current version December 31, 2018.

Digital Object Identifier 10.1109/ACCESS.2018.2883410

Remote Sensing Image Registration Based on Phase Congruency Feature Detection and Spatial Constraint Matching

WENPING MA[1], (Member, IEEE), YUE WU[2], SHAODI LIU[1], QINGXIU SU[1], AND YONG ZHONG[1]

[1]Key Laboratory of Intelligent Perception and Image Understanding, Ministry of Education, School of Artificial Intelligence, Xidian University, Xi'an 710071, China
[2]Xi'an Key Laboratory of Big Data and Intelligent Vision, School of Computer Science and Technology, Xidian University, Xi'an 710071, China

Corresponding author: Yue Wu (ywu@xidian.edu.cn)

This work was supported in part by the Project supported by the Foundation for Innovative Research Groups of the National Natural Science Foundation of China under Grant 61621005, in part by the National Natural Science Foundation of China under Grant U1701267 and Grant 61702392, in part by the China Postdoctoral Science Foundation under Grant 2018T111022 and Grant 2017M623127, in part by the Fundamental Research Funds for the Central Universities under Grant JB181704 and Grant JBX170311, and in part by the International Research Center for Intelligent Perception and Computation, Xidian University.

ABSTRACT In this paper, a novel remote sensing image registration method based on phase congruency (PC) and spatial constraint is proposed. PC can provide intrinsic and meaningful image features, even when there are complex intensity changes or noise. Image features will be well detected from the corresponding PC images by the SAR-SIFT operator. It means that the feature detection methods in the frequency domain (PC) and the spatial domain (SAR-SIFT operator) are combined. To further improve the result of registration, spatial constraints, including point and line constraint, are established by utilizing the position and orientation information. Then, one to more matches can be removed and the influence of adjacent point can be greatly eliminated. The experimental results demonstrate that our method can obtain a better registration performance with higher accuracy and more correct correspondences than the state-of-the-art methods, such as SIFT, SAR-SIFT, SURF, PSO-SIFT, RIFT, and GLPM.

INDEX TERMS Phase congruency, spatial constraint, SAR-SIFT operator, remote sensing, image registration.

I. INTRODUCTION

Remote sensing image registration is a process of aligning images of the same scene which are acquired under different conditions, such as different times, various viewpoints or different sensors [1]–[3]. It is a vital fundamental step of many applications such as image fusion [4], [5], 3-D reconstruction [6], change detection [7], and so on.

Many methods have been developed for remote sensing image registration. They are mainly divided into two groups: area-based and feature-based methods [8], [9]. Area-based methods directly rely on the pixel intensities in the overlapped area to get the geometric transformation model with a certain similarity measure [10], [11]. Cross correlation (CC) [12] and mutual information (MI) [13] are two most well-known area-based methods. Area-based methods avoid complex feature extraction steps, but they are easily influenced by violent illumination changes or noise. Also, the computational complexity of area-based methods is very high.

Compared with area-based methods, feature-based methods will extract features such as points, lines [14], curve and edges. And these methods need to establish reliable feature correspondences first according to the similarities of the descriptors [15], then features are utilized to estimate the geometric transformation between two images. Feature matching is an important step which affects the performance of registration approaches [16], [17]. Feature-based methods are more robust and have higher precision and effectiveness [18]. And feature-based methods can work well when there is complex geometric deformation between two images. Therefore this kind of method is more widely used in remote sensing image registration. In this paper, we mainly study the feature-based methods. Scale-invariant feature transform (SIFT) is one of the commonly used feature-based methods [19].

Gaussian scale space is built to find keypoints. It is invariant to scale changes, rotation, translations and robust to illumination changes and affine distortions. Wang *et al.* [20] introduced a novel bilateral filter SIFT (BFSIFT) method, which uses bilateral filter to build the anisotropic scale space (ASS). ASS can provide more details at coarser scales and more precise location. Delliinger *et al.* [21] developed a SIFT-like (SAR-SIFT) algorithm for SAR images registration, which gives a new gradient computation method. SAR-SIFT is actually based on multiscale Harris algorithm. Ma *et al.* [22] proposed a robust point matching method called PSO-SIFT which utilizes the position, scale, orientation information to redefine the Euclidean distance, and rematches to increase correct correspondences. Fan *et al.* [23] proposed an improved SAR image registration method (LDSR) which directly uses neighborhood intensity information to construct the local descriptors and obtains correspondences by spare representation. Fischler and Bolles [24] proposed a robust sample consensus judging algorithm (RSCJ) and embedded it into random sample consensus (RANSAC). This algorithm can identify bad samples efficiently and dramatically reduce the computational load. Wu *et al.* [25] developed a new point-matching algorithm called fast sample consensus (FSC), which has higher efficiency and stability than RANSAC. Chen *et al.* [26] proposed a robust feature matching method for SAR and optical images by using Gaussian-Gamma-Shaped (GGS) bi-windows-based descriptor and geometric constraint. Li *et al.* [27] proposed a novel feature matching algorithm called RIFT which uses MIM instead of gradient for feature description and achieves rotation-invariant by construction of multiple MIMs. Ma *et al.* [28] proposed a robust guided locality preserving matching (GLPM) for remote sensing image registration. This method is able to handle outliers extremely and can significantly improve the true matches without sacrificing accuracy.

Many feature-based registration methods take advantage of the gray or gradient information to detect the keypoints and get the corresponding descriptors in spatial domain. Such methods are easily affected by illumination, contrast and noise. These factors will make the keypoints unstable and imprecise. Due to the noise, some points will be wrongly detected as keypoints, and some keypoints may not be detected. More importantly, the descriptors will be affected. Then the descriptors cannot correctly express the features of the keypoints. Thus we sometimes cannot find enough correct correspondences or ensure high location accuracy. There are still many practical problems and challenges in remote sensing image registration. Aimed at these problems, phase congruency is applied to image registration in frequency domain. PC is not affected by image illumination and contrast, and robust to speckle noise, and PC also provides rich texture, edge and structural information which is in accordance to human vision [29], so PC has a strong advantage in feature detection [30]. Moreover, to reduce the possibility of mismatch, the spatial constraint is widely used in the computer vision community when matching challenging images [31]. The spatial relationship between objects remains approximately the same [32]. The one to more matches and wrong matches caused by similar descriptors can be greatly removed.

In this paper, a novel remote sensing image registration method based on phase congruency and spatial constraint is proposed. First of all, the PC images of the original images are calculated. PC image can fully reflect the structure information and provide rich meaningful features. Then features are extracted from the two corresponding PC images by SAR-SIFT operator. In this way, methods in both spatial and frequency domain are combined together skillfully. The spatial relationship across corresponding images should basically not change. If two keypoints are close enough, correct matching pairs will not be found. Also there are some one to more matches. To remove these incorrect correspondences as much as possible, the spatial constraints are constructed by using the position and orientation information of the corresponding points. The spatial constraint will increase the number of correct correspondences (inliers) and also improve the accuracy.

Motivated by the success of PSO-SIFT [22], PSO-SIFT utilizes the position, scale, orientation information to build a robust joint distance named position scale orientation Euclidean distance (PSOED), and uses PSOED as the distance measure to rematch. The keypoints are matched by the ratio between the distance of the nearest neighbor and that of the second nearest neighbor. The PSOED will be minimized in most cases when the point pairs are correctly matched. In this way, PSO-SIFT increases correct correspondences. However, if two keypoints are close enough, correct matching pairs will not be found. In this paper, the spatial constraints are constructed by using the position and orientation information of the corresponding points. If two points are correct matching points, then the spatial relationship between these points should be consistent from reference image to sensing image. For example, p_{i1}, p_{i2} and q_{j1}, q_{j2} are correct corresponding matching point pairs which are obtained by SAR-SIFT in the first match. If p_i and q_j are correct matching points, their deviation error should be less than d_{th}. The proposed method is not easy to be affected by noise, so spatial constraint is used to find more point pairs, then the second match can increase inliers very well.

The rest of this paper is organized as follows: SAR-SIFT operator and PC is briefly introduced in Section 2. And the novel method based on PC and spatial constraint is presented in Section 3. Then the datasets, evaluation criterion and parameter setting are described in Section 4. The experimental results are illustrated and compared in Section 5. Finally, the conclusion is drawn in Section 6.

II. RELATED WORK

A. SAR-SIFT OPERATOR

Image registration is actually a process of finding a best transformation matrix to map the sensed image to reference image, and minimizing the dissimilarity between the reference image

and the transformed sensed image in the overlapped area [33]. In feature-based methods, the main challenge is to get enough correct corresponding keypoints. Then the transformation matrix can be calculated. The feature-based methods mainly consist of these steps: feature extraction, feature matching, transformation selection and calculation, image resampling. Feature extraction is the fundamental and important part of image registration methods. Here the SAR-SIFT operator is briefly introduced to show the procedure of feature extraction. As for feature matching, Euclidean distance of descriptors is calculated, then nearest neighbor distance ratio (NNDR) strategy is used to build correspondences. Finally RANSAC is adopted to compute the transformation matrix.

SAR-SIFT is a SIFT-like descriptor mainly adapted to SAR images. The SAR-SIFT algorithm consists of three parts: keypoint detection, orientation assignment, and descriptor extraction.

(1) Keypoint detection: Firstly, the SAR-Harris scale space is constructed by computing the logarithmic ratio of the exponentially weighted averages (ROEWA) operator in each image octave [34]. A new gradient computation method called gradient by ratio (GR) which is based on ROEWA is introduced. GR is more suitable to multiplicative noise than gradient by difference because it takes neighborhood information into consideration. Then extreme points are selected as keypoints. The new multiscale SAR-Harris matrix and the new multiscale SAR-Harris function are defined as:

$$C_{SH}(x, y, \alpha) = G_{\sqrt{2}\alpha} \star \begin{bmatrix} (I_{x,\alpha})^2 & (I_{x,\alpha}) \cdot (I_{y,\alpha}) \\ (I_{y,\alpha}) \cdot (I_{x,\alpha}) & (I_{y,\alpha})^2 \end{bmatrix} \quad (1)$$

$$R_{SH}(x, y, \alpha) = det(C_{SH}(x, y, \alpha)) - d \cdot tr(C_{SH}(x, y, \alpha))^2 \quad (2)$$

where α is the scale, $G_{\sqrt{2}\alpha}$ is a Gaussian kernel with standard deviation $\sqrt{2}\alpha$, $\star$ is the convolution operator, $I_{x,\alpha}$ and $I_{y,\alpha}$ are respectively the horizontal and vertical gradients and d is an arbitrary parameter.

(2) Orientation assignment and Descriptor extraction: A circular neighborhood is used to calculate the main orientation histogram for each keypoint. Then the main orientation can be obtained. As for descriptor extraction, a circular neighborhood and log-polar sectors are used. And the GR gradient makes the feature descriptors efficient. This method is invariant to scale and rotation, and has good robustness to the speckle noise.

B. PHASE CONGRUENCY

PC is a frequency-based model that finds keypoints in an image where there is a high degree of order in the Fourier domain. Assume that, $f(t)$ is a one dimensional signal. At location x, $A_n(x)$ and $\phi_n(x)$ are corresponding amplitude component and phase component in the n_{th} sinusoidal component. Yuan [35] developed a measure of phase congruency via Log Gabor wavelets, which is robust to noise and offers good localization. It is defined as:

$$PC = \frac{\Sigma_n W(x) \lfloor A_n(x) \Delta\phi_n(x) - T \rfloor}{\Sigma_n A_n(x) + \epsilon} \quad (3)$$

$$\Delta\phi_n(x) = \cos(\phi_n(x) - \bar{\phi}(x)) - \left|\sin(\phi_n(x) - \bar{\phi}(x))\right| \quad (4)$$

where W(x) weighs for frequency spread. T is a noise threshold. ϵ is a small parameter for avoiding divided by zero [36]. The term $\bar{\phi}(x)$ denotes the weighted mean phase angle. $\lfloor \cdot \rfloor$ indicates to get the integer that is not larger than it.

The values of PC are high at edge and boundary. According to the principle of PC, features like lines and edges are perceived at points where the Fourier components are in phase with each other. That is to say, values of PC are high in these points. Therefore, PC is usually used as a feature detector in image registration. PC's invariance to image illumination and contrast makes it a robust and reliable feature detection method [30]. Some experiments show that the human visual system reacts more strongly to the points of high PC value by some physiological evidence [37], [38]. In this paper, we do not directly select the points of high PC as initial keypoints. Instead, SAR-SIFT operator is used to detect keypoints on PC images. The following section will clearly illustrate the specific implementation process.

C. TRANSFORMATION MODELS

In remote sensing tasks such as image registration, environmental monitoring, and change detection, the relationships between image pairs are typically modeled by rigid, affine, and similarity transformations [39]. However, most remote sensing images are taken by satellites vertically from high altitude. This will lead to translation, rotation, and other transformations between image pairs, and similarity transformation can process common geometric transformation in remote sensing images registration. Therefore, we assume a similarity transformation model which is widely used in the registration of remote sensing images [22]. Similarity transformation consists of four parameters: rotation, scale, and two shifts. Under the similarity transformation model, the correct matching pairs will have the same rotation angle in space, the same scale ratio, the same horizontal shifts, and the same vertical shifts in most cases. In this paper, similarity transformation is used to study the best geometrical transformation method.

III. PROPOSED METHOD

A. FEATURE DETECTION ON PHASE CONGRUENCY IMAGES USING SAR-SIFT OPERATOR

The methods for feature detection are divided into two types: spatial domain methods and frequency domain methods. Feature detection algorithms based on spatial domain are usually realized by gradient operators such as Sobel, Laplace and Log. In the spatial domain, these gradient operators are used to calculate the gray transformation to detect the features. This kind of method is easy to implement with fast speed, but it is easily affected by illumination, contrast, especially speckle noise, which leads to a large number of unreliable

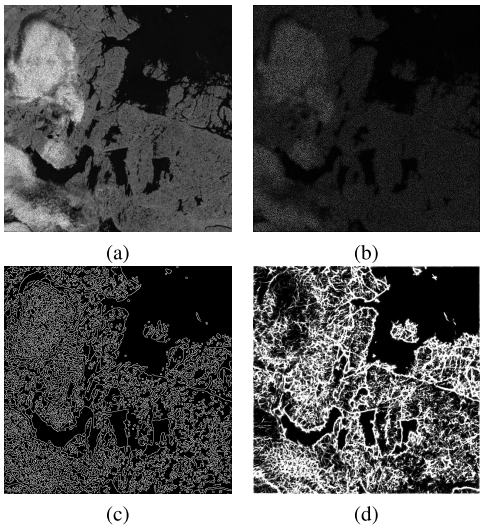

FIGURE 1. Comparsion of features detected by several operators. (a) Image with speckle noise. (b) Laplace. (c) Canny. (d) PC.

keypoints appearing within the initial keypoints. These unreliable keypoints will lead to inaccurate correspondences and further affect the correct calculation of the transformation parameters. While in the frequency domain, Fourier transform is mainly used like phase congruency. It has been proved that phase congruency is invariant to illumination and contrast condition [29], and robust to noise in frequency domain. Also, it offers accurate feature positioning. In view of this, phase congruency model is used to extract feature points in remote sensing images to reduce the influence of wrong and unstable feature points in images. In this paper, we consider the problem from another point of view, and features are extracted on PC images rather than original images. Due to the excellent characteristics of phase congruency, rich and reliable structure information can be obtained. Then the features can be efficiently extracted by SAR-SIFT operator, thus realizing the combination of space domain method and frequency domain method for feature detection.

A simple comparison in Fig. 1 is conducted to illustrate the robustness of PC to noise. The multiplicative noise with a mean of 0 and a variance of 0.04 is added to the image. Laplace, Canny and Phase congruency operators are used as contrast algorithms to detect the features. It can be seen from Fig. 1 that Laplace operator is most sensitive to noise, even the noise is treated as image features to be detected, and the edges are not clear or continuous. As for Canny operator, it will denoise the image with the Gaussian filter, thus this method is not affected by noise. But after filtering, the image becomes blurred and the feature details are lost, which reduces the detection accuracy. As for phase congruency, no filtering is needed. PC can acquire not only features but also internal structure information of the images. As shown, PC is most robust to noise. We also make the same comparison in the real images and the results are shown in Section 5.

PC provides rich texture, edge and structural information. This is consistent with the human visual system's cognition of image features [40]. Owing to these characteristics of PC, the number of feature points obtained by this method is much more than that of the traditional methods which get feature points on original gray images. Sometimes we even cannot get enough correct correspondences on original gray image, thus getting the wrong registration result. But our method can still work well under such condition.

Here the main process of our method is introduced. First of all, phase congruency of every point in two images is calculated. Then SAR-Harris detector as introduced in SAR-SIFT is used to detect keypoints on PC images. In the next step, the dominant orientations of the points are assigned and descriptors are extracted as in SAR-SIFT. After the image descriptors of the keypoints in two images are obtained, NNDR is used to establish feature correspondences. The threshold d_{ratio} is set to 0.9 in experiment. After that, RANSAC is used to obtain the optimal transformation model parameters and get the correct matching pairs at the same time. Finally, we obtain the initial correct matching point pairs and the transformation matrix.

By the way, in order to reduce the computational complexity, we only choose a part of initial keypoints before feature matching. Similar to structural similarity (SSIM) [41], the criterion for preselection is defined as:

$$\rho(P_R(r_m), P_S(s_n)) = \frac{2\mu_R(r_m)\mu_S(s_n)}{[\mu_R(r_m)]^2 + [\mu_S(s_n)]^2} \times \frac{2\sigma_R(r_m)\sigma_S(s_n)}{[\sigma_R(r_m)]^2 + [\sigma_S(s_n)]^2} \quad (5)$$

where $P_R(r_m)$ means the image patch in the reference image centered at the feature point r_m, $P_S(s_n)$ indicates the image patch in the sensed image centered at the sensed point s_n, $\mu_R(r_m)$ and $\sigma_R(r_m)$ are the intensity mean and standard deviation in image patch $P_R(r_m)$. Likewise, $\mu_S(s_n)$ and $\sigma_S(s_n)$ are the intensity mean and standard deviation in image patch $P_S(s_n)$. If $\rho \leq \rho_{th}$, then the sensed point s_n can be regarded as the potential match of r_m. Many impossible matching points are removed by this way to avoid unnecessary calculation.

In view of the characteristic of PC, features are detected on corresponding PC images by SAR-SIFT operator. The influence of noise can be reduced as much as possible. But one to more matches and wrong matches are still inevitable. Multiple orientations and adjacent keypoints all could lead to this situation. And then spatial constraint is used to solve these problems.

B. INCREASE CORRECT CORRESPONDENCES USING SPATIAL CONSTRAINT

An enhanced feature point matching strategy called spatial constraint is proposed to greatly increase the number of correct matching points (inliers). If two points are correct matching points, then the spatial relationship between these points should be consistent from reference image to sensing image. PC is robust to noise, we can largely reduce its influence. But there are some close enough keypoints, these points will have similar descriptors. Thus some potential correct matching

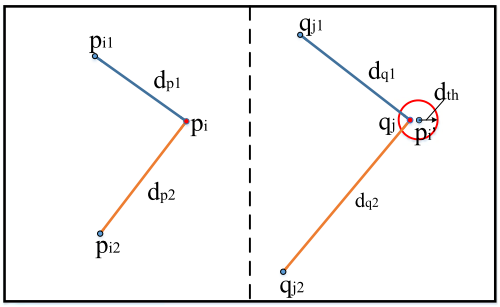

FIGURE 2. Spatial constraint between two images. p_{i1}, p_{i2} and q_{j1}, q_{j2} are correct corresponding matching point pairs which are obtained in the first match. If p_i and qj are correct matching points, their deviation error should be less than d_{th} (Point constraint), and $r_d = \frac{d_p}{d_q}$ should be approximately a constant (Line constraint).

points cannot be found by NNDR. Also, there are some one to more matches or even wrong matches. The spatial constraint is not easy to be affected by noise, so spatial constraint is used to find more point pairs, then the second match can increase inliers very well.

Two initial keypoint sets $P = \{p_1, p_2, ...p_m\}$ and $Q = \{q_1, q_2, ..., q_n\}$ have been acquired after NNDR. (x_i, y_i) and θ_i indicate the position and dominant orientation of i_{th} keypoint in the reference image. Similarly, (x'_j, y'_j) and θ_j indicate the position and dominant orientation of j_{th} keypoint in the sensed image. The point set P_C and Q_C represent the match pairs filtered by RANSAC. And the mapped point (x''_j, y''_j) of original point (x'_j, y'_j) in the sensed image is obtained by transformation matrix. Think of the spatial constraint from two perspectives: Point and Line. Specifically, the correct match pairs should have the same main orientation error and the unchanged distance ratio. These spatial constraints go forward one by one, gradually reduce the scope, and finally get the exact results.

(1) Point constraint: Firstly, the main orientation error for each correct correspondence should be basically same. $e_\theta(i, j)$ is the main orientation error between the two points (p_i and q_j) to be judged, and $\bar{\theta}_C$ is the average main orientation error between P_C and Q_C. By this way, on the basis of the results which we have obtained, we choose the potential point pairs from the original keypoint sets. We set a threshold θ_{th}, then the main orientation error and main orientation constraint can be defined as:

$$e_\theta(i, j) = \left|\theta_i - \theta_j\right| \quad \left|e_\theta(i, j) - \bar{\theta}_C\right| \le \theta_{th} \tag{6}$$

Secondly, the correct corresponding keypoints should locate in the same position in the corresponding image. Considering the unavoidable error of the point coordinates, the deviation error between each correct corresponding points should be less than a threshold d_{th}. By so doing, the range of possible matching pairs is further narrowing. The deviation error of p_i and q'_j is defined as:

$$e_d(i, j) = \sqrt{(x_i - x''_j)^2 + (y_i - y''_j)^2} < d_{th} \tag{7}$$

(2) Line constraint: If p_{i1} in set P_C and q_{j1} in set Q_C are one correct match pair which is regarded as a benchmark for judgment. There are two points p_i in set P and q_j in set Q to be judged. The distance between p_{i1} and p_i is called d_{p1}. Similarly, the distance between q_{j1} and q_j is called d_{q1}. If this two points p_i and q_j are a correct match pair, the distance ratio $r_d = \frac{d_{p1}}{d_{q1}}$ should be a constant. This is called the distance ratio invariant criterion. In the experiment, the distance ratio invariant criterion is used to get the final precise results.

$$r_d = \frac{\sqrt{(x_{i1} - x_i)^2 + (y_{i1} - y_i)^2}}{\sqrt{(x'_{j1} - x'_j)^2 + (y'_{j1} - y'_j)^2}} \tag{8}$$

The geometric relationship between matching features should not change too much across images. Point constraint and line constraint are effective and reliable even if there are violent illumination changes or noise. More importantly, when some descriptors cannot fully express the difference between features of the keypoints, spatial constraint can still work. For this reason, we can increase reliable matching point pairs.

IV. DATASET, EVALUATION CRITERION AND PARAMETER SETTING

A. DATASET

To evaluate the effectiveness and accuracy of our method, four image pairs are tested. These image pairs are shown in Fig. 3. Similarity transform model is used for the geometric distortion between image pairs.

(1) Image pair 1: The first pair includes two 614×611 multispectral images form USGS project, Lat/Long: 69.6/-92.7, 240-m resolution. The reference image is from band 5(Sensor: Landsat-7 ETM+, Date: 2000/7/24). The sensed image is from Band 3 (Sensor: Landsat 4-5 TM, Date: 1999/6/28). There are violent and irregular gray changes between two images.

(2) Image pair 2: The second pair includes two 256×256 multisensor images of the same area (an urban area in Brasilia, Brazil). While reference image is band 3 from a scene taken by SPOT on August 8, 1995. Sensed image is band 4 from a scene by the sensor Landsat Thematic Mapper (TM) on June 07, 1994.

(3) Image Pair 3: The third pair includes two 400×400 images from different looks. Reference image is a single-look SAR image and sensed image which contains more noise is a four-look SAR image. They were taken in June 2008 and June 2009 by Radarset-2 (C band) at the region of Yellow River Estuary, respectively. The spatial resolution is 8 m.

(4) Image Pair 4: The fourth pair includes two 400×400 SAR images of same places (Wuhan, China)

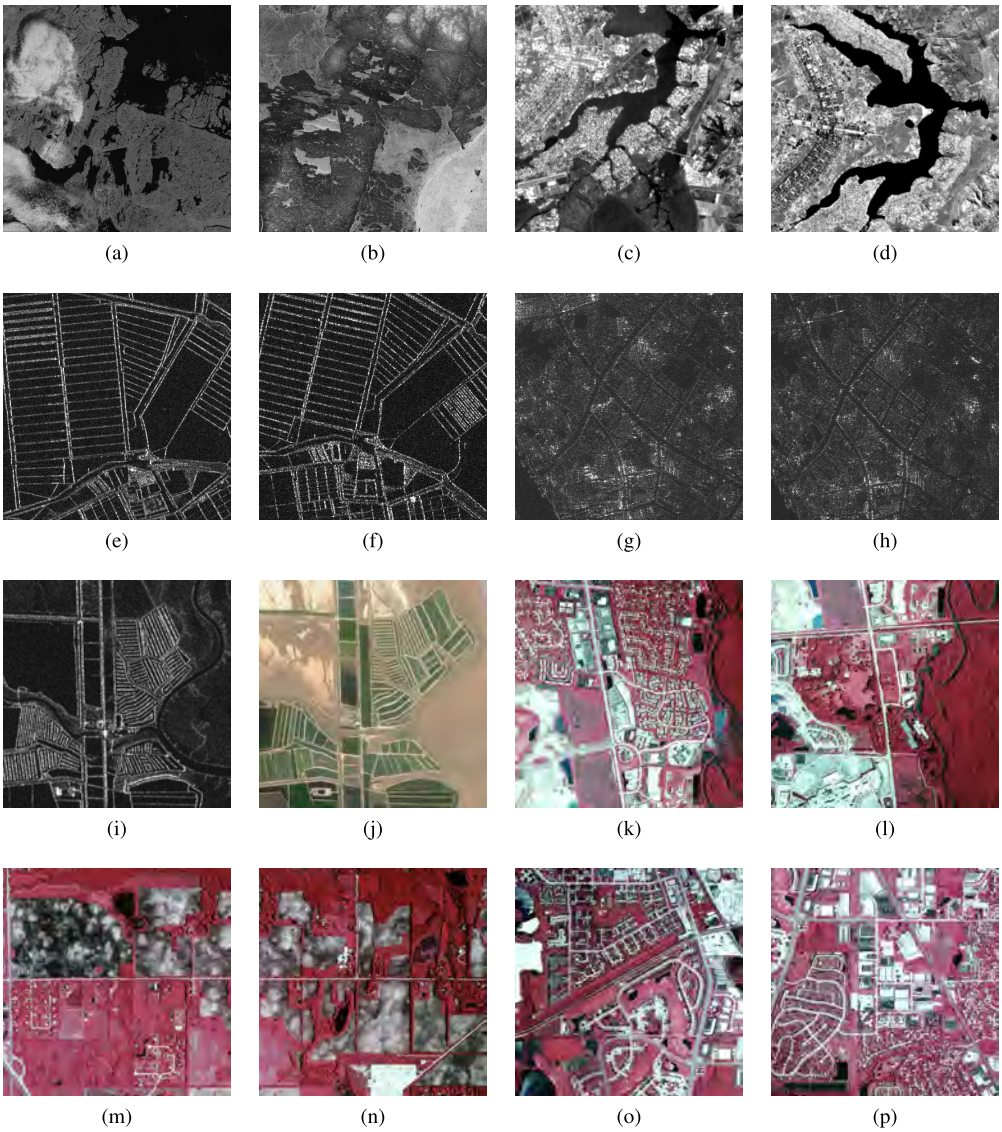

FIGURE 3. Remote sensing image pairs. (a)(b) Landsat-7 ETM+, band 5. (c)(d) Landsat 4-5 TM, band 3. (e)(f) SPOT, band 3. (g)(h) TM, band 4. (i) Radarsat-2, C-band. (j) Google Earth. (k)-(p) Erdas example data.

by ALOS-PALSAR. They were taken in June 04, 2006 and March 07, 2009, respectively. The spatial resolution is 10 m.

(5) Image pair 5: The fifth pair includes one SAR image of size 463×413×1 and one optical image of size 463×413×3. The SAR image is the C-band of the Radarsat-2 image acquired in June 2008, whereas the optical image is acquired from Google Earth in September 2012, including red, green, and blue bands. This dataset records the changes of land use in Shuguang Village, Dongying City, China. The spatial resolution is 8 m.

(6) Image pair 6, 7, and 8: The three pairs are all of size 700×700 and have already been rectified, and hence, undergo just rigid transformation. The feature matching task for such image pairs typically arises in the image mosaic problem. The images are publicly available (from the Erdas example data), which were captured over eastern Illinois, IL, USA.

B. EVALUATION CRITERION

(1) Root-Mean-Square Error (RMSE): RMSE [8] is computed to evaluate the accuracy. The RMSE is defined as:

$$RMSE = \sqrt{\frac{1}{N}\sum_{i=1}^{N}(x_i - x_i'')^2 + (y_i - y_i'')^2} \qquad (9)$$

where (x_i'', y_i'') means the transformed coordinates of (x_i', y_i'). N means the total number of correct matching pairs. To reduce the error, the algorithm is repeated for

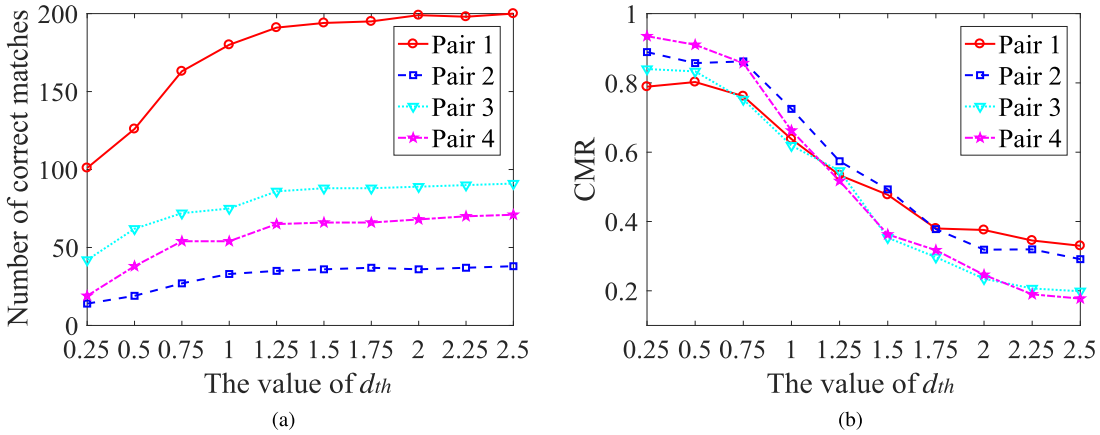

FIGURE 4. Experimental results of these image pairs with different values of d_{th}. (a) The number of correct matches. (b) The rate of correct matches (CMR).

TABLE 1. Compare of RMSE, Number of correct matches, and Time of test image pairs.

Operator		Laplace	Canny	PC
Image Pair 2	RMSE	0.5840	0.4480	**0.5123**
	N	29	10	**37**
	T	9.512	9.567	**9.450**
Image Pair 3	RMSE	0.5238	0.5019	**0.4900**
	N	57	39	**86**
	T	40.325	43.593	**29.88**

five times and the average value is regarded as the final RMSE.

(2) Number of correct matches (N): The number of correct correspondences is used as the criterion to evaluate the robustness of the proposed method. The correct matching correspondence denotes the matched points which have been filtered by spatial constraint and RANSAC as inliers.

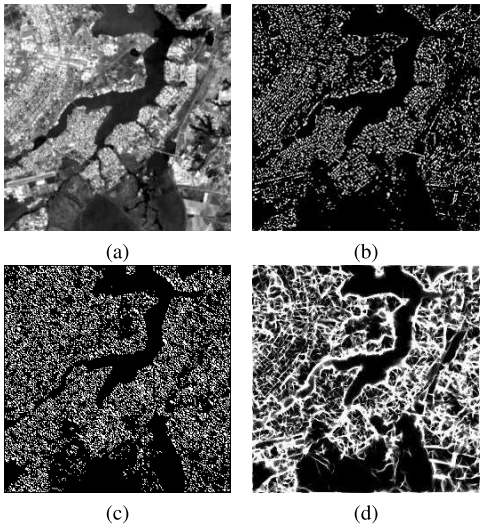

FIGURE 5. Comparsion of features detected from reference image of image pair 2. (a) The original image. (b) Laplace. (c) Canny. (d) PC.

C. PARAMETER SETTING

When SAR-SIFT operator is used to detect features on PC images, we keep the same parameter settings of the relative parameters such as the first scale α, the arbitrary parameter of the SAR-Harris criterion d, and so on. In the preselection procedure, an empirical value of 0.9 is suggested for ρ_{th}. Only the neighborhood paths of two corresponding keypoints are similar enough, this pair keypoints are considered as potential matches. This means that we do not need to spend time on the impossible keypoint pairs whose neighborhood paths are quite different. As for the procedure of second match, the main orientation error threshold θ_{th} is set to 4. It is an experimental value because we only take the correct correspondences of the first match into account up to present. The main orientation constraint can narrow the search scope, and it does not need to be very accurate. The deviation error constraint is utilized to get more accurate results. The deviation error threshold d_{th} is very important to get enough correct matching correspondences and ensure the accuracy at the same time. From Fig. 4, we can know that the number of correct matches increases first and then basically remains unchanged with the d_{th}, while the rate of correct matches decreases. To ensure the rate of correct matches (CMR) and get enough correct matches at the same time, d_{th} is set to 1.25.

V. EXPERIMENT RESULTS

A. NOISE ROBUSTNESS TEST

We use the real images without manually added speckle noise as contrasts to illustrate the robustness of phase congruency to noise. Fig. 5 and Fig. 6 are the comparisons of the results of the detected features. And the matching accuracy (RMSE), Number of correct matches (N), and Time (T) of different operators are listed in the Table 1.

TABLE 2. Compare of RMSE, Number of correct matches, and Time of test image pairs (+: uses spatial constraints *: fails to get correct registration result).

Method		SIFT	SIFT+	SAR-SIFT	SAR-SIFT+	SURF	SURF+	RSCJ	LDSR	PSO-SIFT	RIFT+	GLPM+	**Proposed**
Pair1	RMSE	*	*	*	*	*	*	*	*	0.6021	*	*	**0.5631**
	N	*	*	*	*	*	*	*	*	155	*	*	**192**
	T	16.79	22.735	20.47	25.335	5.52	7.43	15.25	89.15	29.19	8.504	0.0885	**60.94**
Pair2	RMSE	0.5246	0.5267	*	*	0.5341	0.5408	0.7261	*	0.6192	1.6878	*	**0.5123**
	N	13	18	*	*	8	9	17	*	22	26	*	**37**
	T	7.02	18.4476	6.10	8.405	2.94	3.546	3.73	13.24	6.12	3.275	0.0242	**9.45**
Pair3	RMSE	0.523	0.4696	0.5796	0.4088	0.4431	0.5063	0.8655	0.5432	0.5889	*	*	**0.4900**
	N	13	19	35	63	4	6	20	15	44	*	*	**86**
	T	5.63	5.678	14.89	16.866	4.43	5.332	4.56	58.67	18.15	8.08	0.0429	**29.88**
Pair4	RMSE	0.4188	0.585	0.4522	0.4357	0.6111	0.6224	0.5867	0.3671	0.5511	1.6400	*	**0.5090**
	N	5	6	8	59	16	19	5	4	8	37	*	**67**
	T	6.54	7.516	6.72	13.926	3.89	4.125	4.16	27.06	7.06	4.613	0.0334	**20.54**
Pair5	RMSE	0.2827	0.3283	0.1264	0.1950	*	*	*	0.5174	0.7005	1.1883	*	**0.5512**
	N	4	6	3	11	*	*	*	8	8	11	*	**71**
	T	6.617	7.510	8.144	19.787	3.678	4.248	6.464	32.442	6.300	5.693	0.146	**40.045**
Pair6	RMSE	0.1299	0.1299	0.2228	0.3040	0.3972	0.3886	0.3577	0.1899	0.1529	0.2693	0.2661	**0.1676**
	N	209	209	76	80	113	116	80	54	172	41	850	**268**
	T	34.081	56.157	37.895	49.504	15.291	18.793	36.214	43.209	135.979	10.627	0.615	**294.43**
Pair7	RMSE	0.0587	0.0587	0.2280	0.2313	0.1766	0.1408	0.2790	0.2013	0.1645	0.3763	0.2421	**0.2030**
	N	235	235	74	83	144	145	75	47	220	48	527	**260**
	T	32.765	45.739	31.547	37.112	9.984	12.168	29.767	45.7	81.79	10.168	0.634	**290.665**
Pair8	RMSE	0.0815	0.0815	0.1554	0.1717	0.2137	0.1865	0.2174	0.1884	0.0949	0.2450	0.1915	**0.1783**
	N	221	221	117	120	192	197	122	86	175	81	855	**283**
	T	58.595	74.658	88.679	90.479	18.939	24.981	58.526	78.709	215.763	9.453	0.953	**454.241**

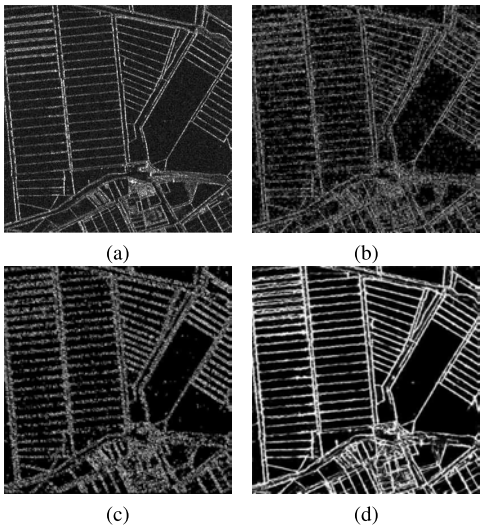

FIGURE 6. Comparsion of features detected from reference image of image pair 3. (a) The original image. (b) Laplace. (c) Canny. (d) PC.

It can be seen from Fig. 5 and Fig. 6 that Laplace operator and Canny operator are most sensitive to noise, and the edge features detected by PC are clear and continuous. Overall, the performance of features extracted by Canny operator is better than that of Laplace operator. That's because the Canny operator uses the Gaussian filter to reduce noise. PC provides rich texture, edge and structural information, thus PC can acquire not only features but also internal structure information of the images. And we utilize PC to detect features in order to obtain better performance of registration with higher accuracy and more correct correspondences.

From the Table 1, we can see that PC obtains better RMSE, more number of correct matches and spends less time. PC is able to provide rich texture, edge, and structural information. Owing to these characteristics of PC, the number of feature points obtained by this method is much more than that of the traditional methods which get feature points on original gray images. Sometimes we even cannot get enough correct correspondences on original gray image to get the wrong registration result. But our method can increase reliable matching point pairs and still work well in this case. So PC is most robust to noise.

B. REGISTRATION PERFORMANCE TEST

We compare the proposed method with the SIFT [42], SAR-SIFT [21], SURF [43], RSCJ [44], PSO-SIFT [22], LDSR [23], RIFT [27], GLPM [28] algorithms, and to be fair, we add spatial constraints to SIFT, SAR-SIFT, SURF, RIFT, and GLPM algorithms. SIFT is a most representative method. SIFT and SIFT-based methods like SURF, PSO-SIFT have been widely used in remote sensing image registration. SAR-SIFT has good performance on SAR image registration. There are several SAR image pairs in our dataset. And the contrastive experiment results will prove the advantage

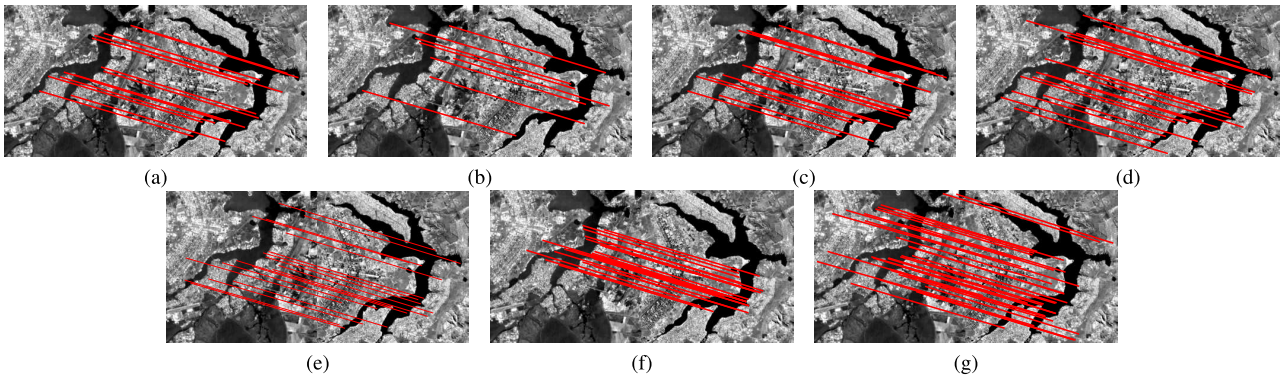

FIGURE 7. Matching results of pair 2: (a) SIFT. (b) SURF. (c) RSCJ. (d) PSO-SIFT. (e) SIFT+. (f) RIFT+. (g) The proposed method.

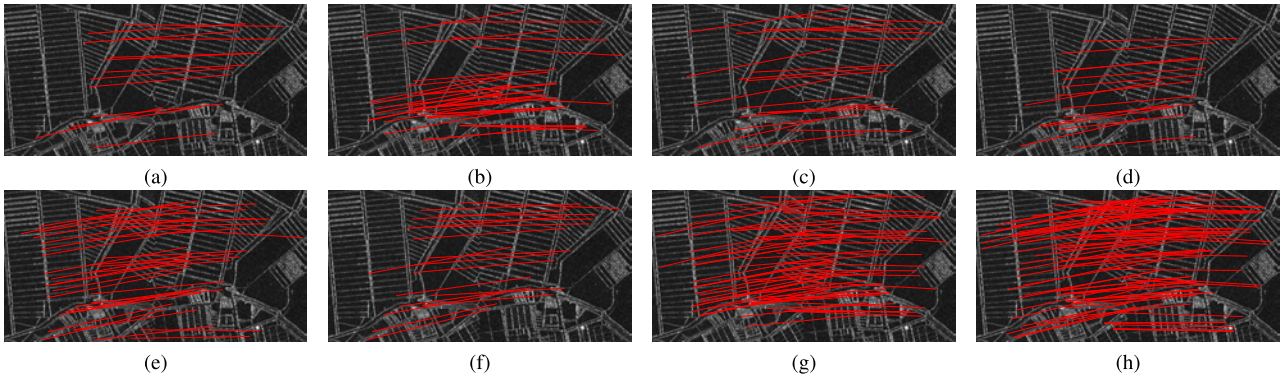

FIGURE 8. Matching results of pair 3: (a) SIFT. (b) SAR-SIFT. (c) RSCJ. (d) LDSR. (e) PSO-SIFT. (f) SIFT+. (g) SAR-SIFT+. (h) The proposed method.

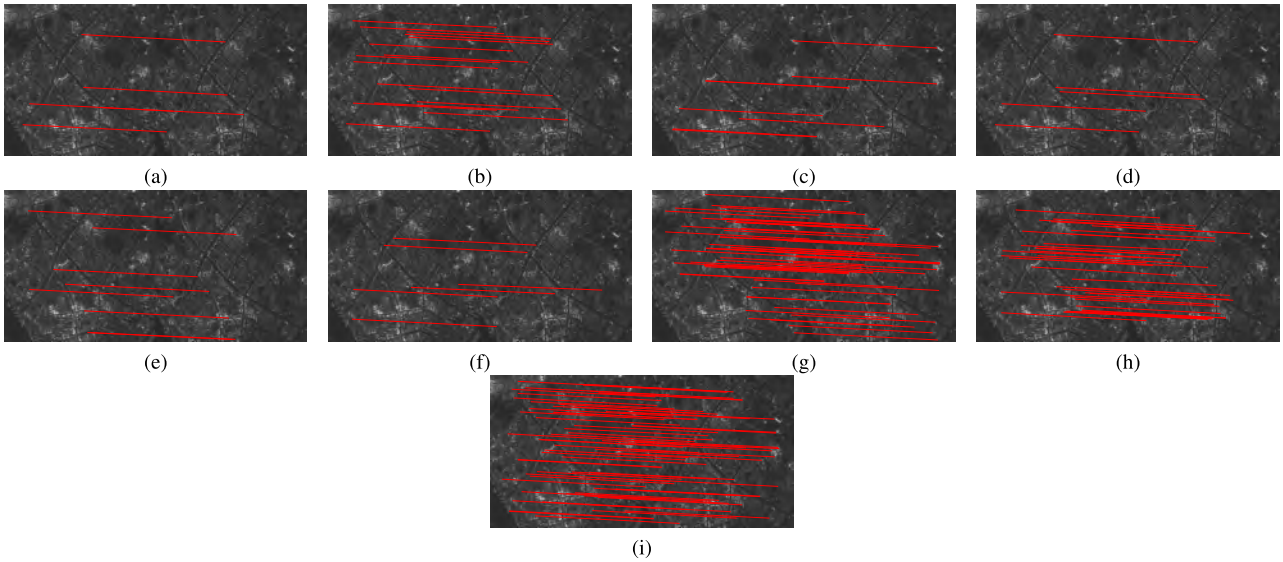

FIGURE 9. Matching results of pair 4: (a) SIFT. (b) SURF. (c) SAR-SIFT. (d) RSCJ. (e) PSO-SIFT. (f) SIFT+. (g) SAR-SIFT+. (h) RIFT+. (i) The proposed method.

of our method. As for LDSR, it constructs the descriptors with intensity and geometric information of image patches rather than gradient information. This method actually can only get good results when two images are similar enough and it usually suffers from geometry deformation and gray distortion. Similarly, our method does not directly use gray gradient information either. The descriptors are extracted on PC images. RSCJ is a method which is used in feature matching stage. RIFT has rotation invariance and is suitable for a variety of multi-modal remote sensing images. And GLPM is a novel mismatch removal method for robust feature matching of remote sensing images. It works based on a

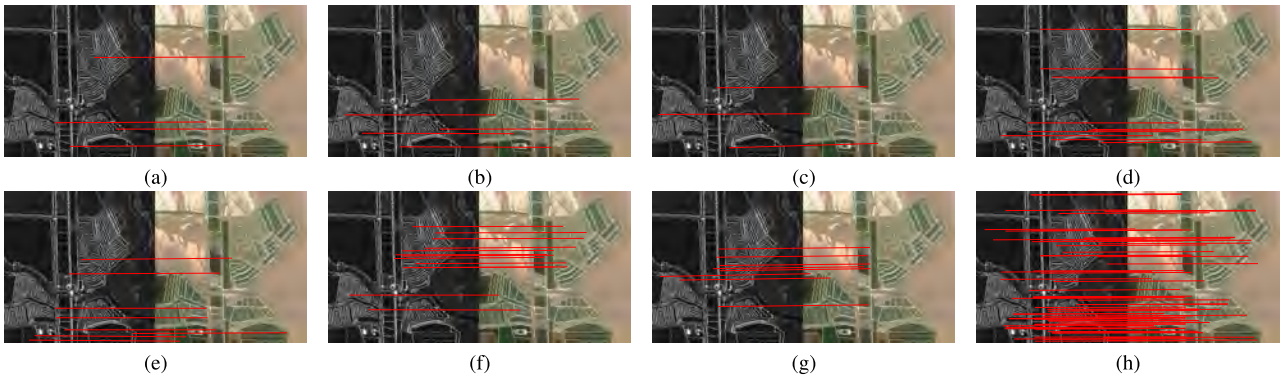

FIGURE 10. Matching results of pair 5: (a) SIFT. (b) SIFT+. (c) SAR-SIFT. (d) SAR-SIFT+. (e) LDSR. (f) RIFT+. (g) PSO-SIFT. (h) The proposed method.

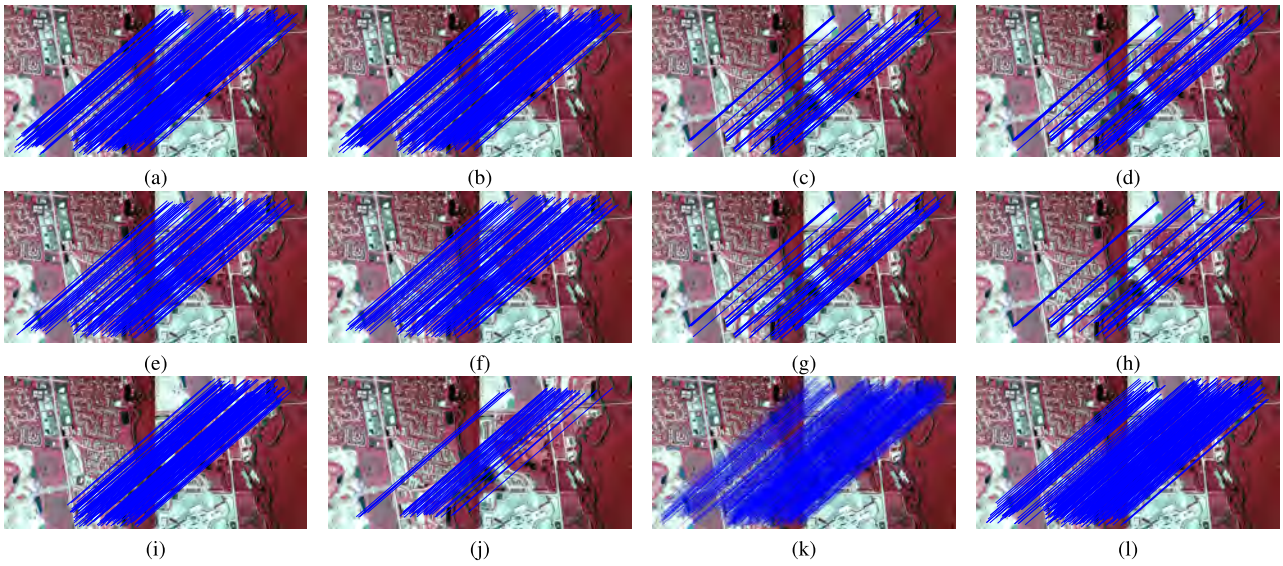

FIGURE 11. Matching results of pair 6: (a) SIFT. (b) SIFT+. (c) SAR-SIFT. (d) SAR-SIFT+. (e) SURF. (f) SURF+. (g) RSCJ. (h) LDSR. (i) PSO-SIFT. (l) RIFT+. (k) GLPM+. (l) The proposed method.

general characteristic that the neighborhood structures of feature correspondences between two images of the same scene should be similar. Experimental results show that our method has a better performance than these traditional methods for remote sensing image registration.

The matching results and the mosaiced images for eight image pairs are shown in Fig. 7-14. And the matching accuracy (RMSE), Number of correct matches (N), and Time (T) are listed in Table 2. Owing to the adoption of phase congruency and spatial constraint, our method can get better result.

Image pair 1 and 2 are obtained in two different bands from different sensors. So the intensity mapping relation between these two images is complex. Common methods are usually ineffective in this situation. The results in Table 2 indicate that SIFT, SURF, SAR-SIFT, RSCJ, LDSR, RIFT, and GLPM all fail to get right registration result for pair 1. The descriptors of these methods are seriously influenced by significant difference of the image intensity. So the descriptors of compared methods may not well express the features. Then the distance of corresponding feature descriptors will not measure the real relation of two corresponding points. Therefore, these methods cannot obtain enough reliable correspondences to compute the transformation matrix parameters. But our method considers this question from another perspective. Two images are registered on PC images by SAR-SIFT operator. PC images provide us rich and meaningful texture, edge and structural information. Thus true image features are obtained. As shown, we can get correct and better registration result.

As shown in the Table 2 and Fig. 7, although SIFT, SURF, RSCJ, PSO-SIFT, and RIFT can get match results for image pair 2, the number of correct correspondences is small, and the accuracy is poor. These criteria indicate that common methods may not meet the requirements. Due to the local geometry deformation, gray distortion and different imaging mechanism, it is difficult to get good registration result. The characteristics of PC and spatial constraint play an important role in such circumstances. PC images reflect the internal nature image features to reduce the impact of mentioned influence factors as much as possible. And the spatial constraint is mainly used to remove imprecise keypoints instead

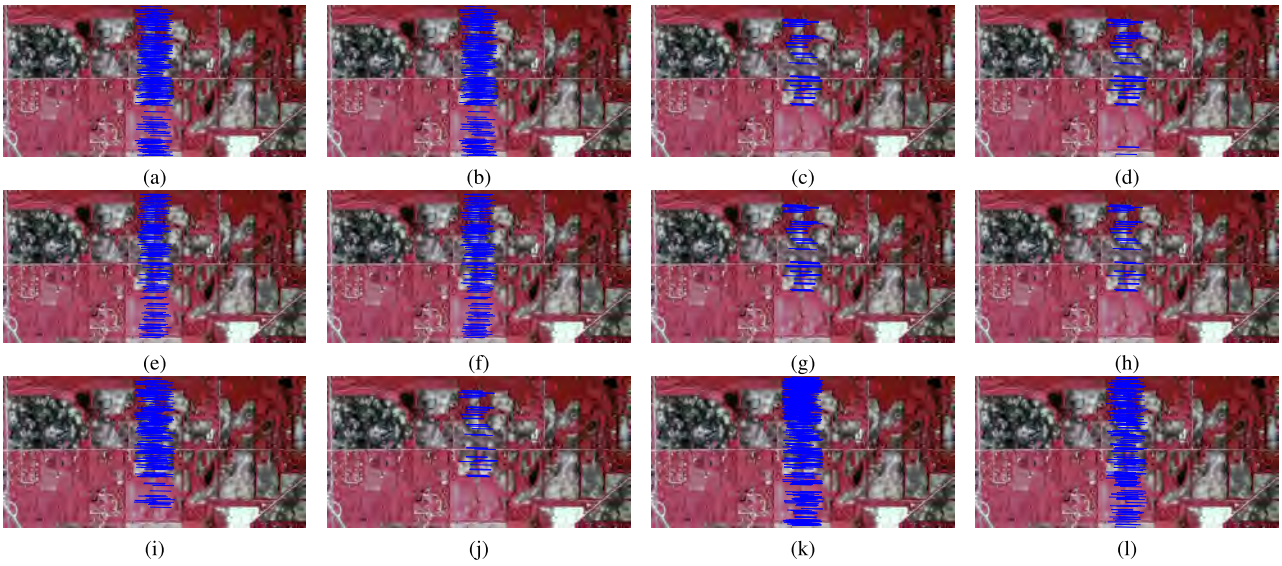

FIGURE 12. Matching results of pair 7: (a) SIFT. (b) SIFT+. (c) SAR-SIFT. (d) SAR-SIFT+. (e) SURF. (f) SURF+. (g) RSCJ. (h) LDSR. (i) PSO-SIFT. (l) RIFT+. (k) GLPM+. (l) The proposed method.

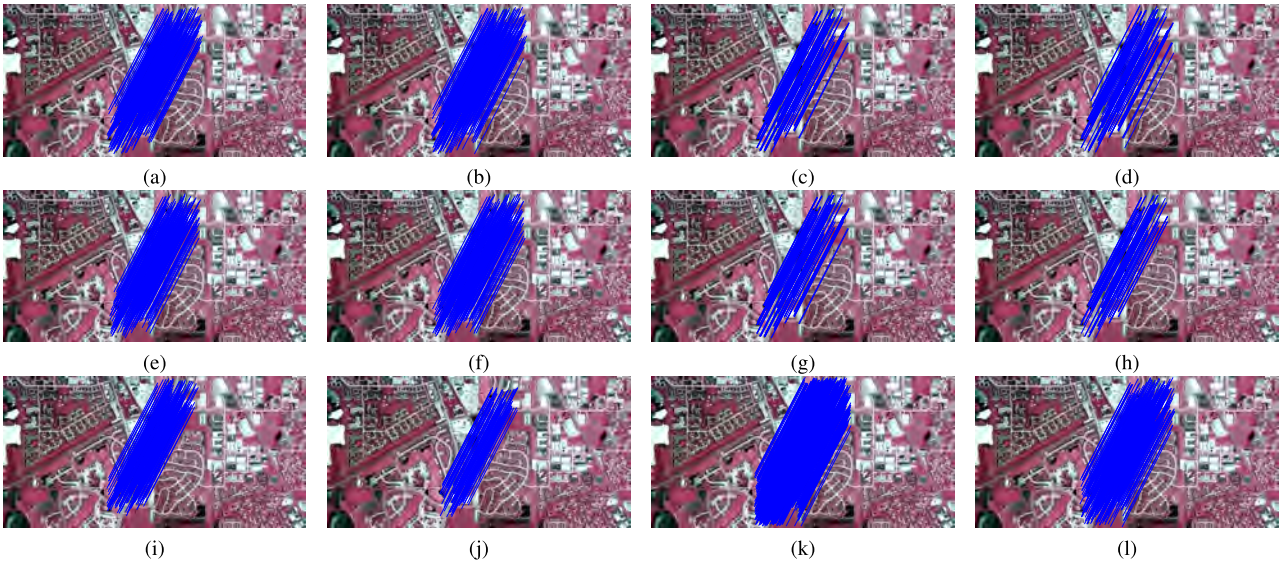

FIGURE 13. Matching results of pair 8: (a) SIFT. (b) SIFT+. (c) SAR-SIFT. (d) SAR-SIFT+. (e) SURF. (f) SURF+. (g) RSCJ. (h) LDSR. (i) PSO-SIFT. (l) RIFT+. (k) GLPM+. (l) The proposed method.

of increasing correct correspondences in this case. Thus our method can get a result with higher accuracy and a little more correct correspondences.

And the Table 2 and Fig. 8 show that all the methods can align image pair 3. But spatial constraint is adopted in our method, and more correct correspondences are obtained. We can see that SIFT, SAR-SIFT, and SURF using spatial constraint can get more correct matches. Number of correct matches in our method is almost two to six times as many as other methods. Many wrong matches are caused by noise or similar pixels around the keypoints. And one to more matches are found because two keypoints are close enough in position or they have similar descriptors. By setting the suitable error thresholds of spatial constraint, these wrong matches can be removed.

As shown in Fig. 9, the compared methods can get the registration result for image pair 4. However, the numbers of correct matches almost are no more than 10. There are lots of speckle noise between this two SAR images. Due to the speckle noise, some real keypoints cannot be found and some pseudo keypoints are regarded as real keypoints. Furthermore, the calculation of gradient and descriptors is influenced. Then only few correct matching pairs are found. But PC images are more robust to noise, and then keypoints and descriptors of our method are more stable and reliable. Therefore, much more correct correspondences are obtained. Moreover, the spatial constraint helps to increase the correct matches.

The registration results for image pair 5 are shown in Fig. 10. Since the SAR image's imaging principle is

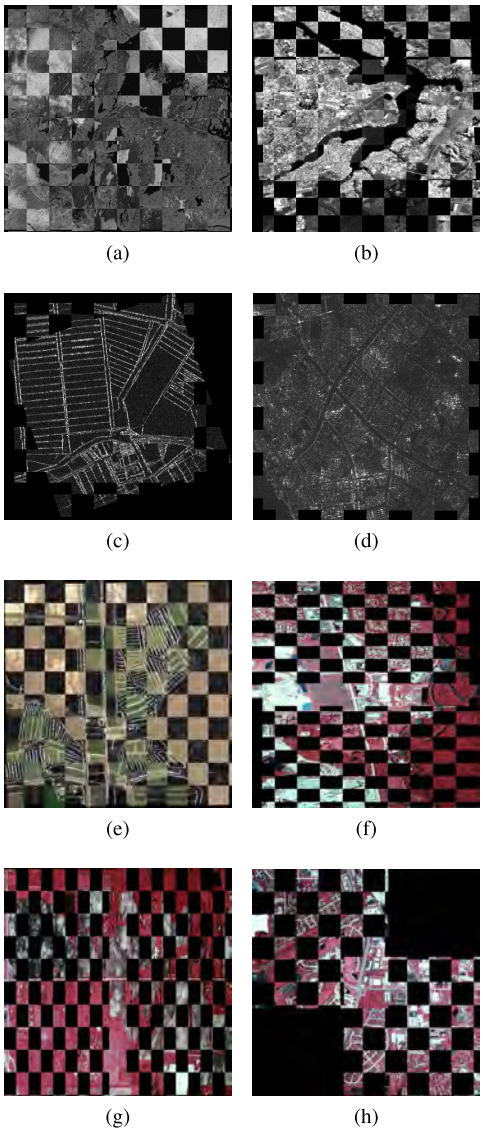

FIGURE 14. Mosaiced images of proposed method: (a) pair 1. (b) pair 2. (c) pair 3. (d) pair 4. (e) pair 5. (f) pair 6. (g) pair 7. (h) pair 8.

very different from the optical image and there is inherent speckle noise, the compared algorithms find only few correct matching pairs. The PC uses location, scale, and orientation information, features are well detected, and the spatial constraint approach also increases the number of potential correct matches. But the spatial constraint requests the higher computational complexity. Our method can get better results than other methods.

And the Table 2 and Fig. 11-13 show that all the methods can align image pair 6, 7, and 8. But spatial constraint is adopted in our method, and more correct correspondences are obtained. Many wrong matches are caused by noise or similar pixels around the keypoints. And one to more matches are found because two keypoints are close enough in position or they have similar descriptors. By setting the suitable error thresholds of spatial constraint, the wrong matches can be removed. However, the proposed method needs to calculate the PC images and construct the spatial constraint relation. Especially when the images with large size have very rich corner and texture information, these steps will lead to unavoidable computation. Because SIFT features are local features of the image, which remain invariant to rotation, scale scaling, and brightness changes. Image pairs 6, 7, and 8 are simply rigid (such as translation and rotation) transformations, and SIFT can extract features well. The first step of GLPM algorithm is to use SIFT to extract features, so SIFT and GLPM can get better matching performance. In addition, GLPM can identify outliers from over 1000 putative matches in only a few milliseconds. All in all, the proposed method is better than other methods except GLPM in these three image pairs.

Furthermore, the Taylor expansion of SAR-Harris scale-space is utilized to achieve sub-pixel accuracy. Although keypoints are preselected before matching, the number of remaining keypoints is still several times as many as the compared methods. And considering the calculation of descriptors and the construction of the spatial constraint, the computational complexity is higher than compared algorithms. The checkerboard mosaiced images are shown in Fig. 14. The overlapped region can been clearly seen.

VI. CONCLUSION

In this paper, a novel registration method based on phase congruency and spatial constraint is introduced for remote sensing image registration. Different from traditional algorithms, we register PC images of the the reference image and sensed image rather than that of the original gray images. Experiments show that this method overcomes the challenge of irregular and complex intensity changes of remote sensing images and can get higher accuracy compared with the state-of-the-art and classic methods. Moreover, spatial constraint is utilized to get more correct matches to improve the registration results. It will remove the wrong or one to more matches and identify the right matching points even there are interfering points just around the point to be matched. But we need to calculate the PC images and construct the spatial constraint relation. Especially when the images with large size have very rich corner and texture information, these steps will lead to unavoidable computation. The computational efficiency needs to be improved in further research.

ACKNOWLEDGMENT

(Wenping Ma and Yue Wu contributed equally to this work.)

REFERENCES

[1] B. Zitová and J. Flusser, "Image registration methods: A survey," *Image Vis. Comput.*, vol. 21, pp. 977–1000, Oct. 2003.

[2] W. Cao, F. Lyu, Z. He, G. Cao, and Z. He, "Multimodal medical image registration based on feature spheres in geometric algebra," *IEEE Access*, vol. 6, pp. 21164–21172, Jan. 2018.

[3] Y. Dong, T. Long, W. Jiao, G. He, and Z. Zhang, "A novel image registration method based on phase correlation using low-rank matrix factorization with mixture of Gaussian," *IEEE Trans. Geosci. Remote Sens.*, vol. 56, no. 1, pp. 446–460, Jan. 2018.

[4] Y. Yang, W. Wan, S. Huang, F. Yuan, S. Yang, and Y. Que, "Remote sensing image fusion based on adaptive IHS and multiscale guided filter," *IEEE Access*, vol. 4, pp. 4573–4582, Jan. 2016.

[5] B. Lin, X. Tao, Y. Duan, and J. Lu, "Hyperspectral and multispectral image fusion based on low rank constrained Gaussian mixture model," *IEEE Access*, vol. 6, pp. 16901–16910, Jan. 2018.
[6] B. Tian, S. Shi, Y. Liu, S. Xu, and Z. Chen, "Image registration of interferometric inverse synthetic aperture radar imaging system based on joint respective window sampling and modified motion compensation," *J. Appl. Remote Sens.*, vol. 9, no. 1, p. 95097, Jan. 2015.
[7] L. Ke, Y. Lin, Z. Zeng, L. Zhang, and L. Meng, "Adaptive change detection with significance test," *IEEE Access*, vol. 6, pp. 27442–27450, Jan. 2018.
[8] M. Gong, S. Zhao, L. Jiao, D. Tian, and S. Wang, "A novel coarse-to-fine scheme for automatic image registration based on SIFT and mutual information," *IEEE Trans. Geosci. Remote Sens.*, vol. 52, no. 7, pp. 4328–4338, Jul. 2014.
[9] J. Ma, J. Zhao, Y. Ma, and J. Tian, "Non-rigid visible and infrared face registration via regularized Gaussian fields criterion," *Pattern Recognit.*, vol. 48, no. 3, pp. 772–784, Mar. 2015.
[10] X. Li, "High-accuracy subpixel image registration with large displacements," *IEEE Trans. Geosci. Remote Sens.*, vol. 55, no. 11, pp. 6265–6276, Nov. 2017.
[11] D. P. L. Ferreira, E. Ribeiro, and C. A. Z. Barcelos, "A variational approach to non-rigid image registration with bregman divergences and multiple features," *Pattern Recognit.*, vol. 55, pp. 237–247, Jan. 2018.
[12] G. Dahman, J. Flordelis, and F. Tufvesson, "Cross-correlation of large-scale parameters in multi-link systems: Analysis using the Box-Cox transformation," *IEEE Access*, vol. 6, pp. 13555–13564, Jan. 2018.
[13] S. Suri and P. Reinartz, "Mutual-information-based registration of TerraSAR-X and Ikonos imagery in urban areas," *IEEE Trans. Geosci. Remote Sens.*, vol. 48, no. 2, pp. 939–949, Feb. 2010.
[14] Y. Yang, S. H. Ong, and K. W. C. Foong, "A robust global and local mixture distance based non-rigid point set registration," *Pattern Recognit.*, vol. 48, no. 1, pp. 156–173, Jan. 2015.
[15] J. Liang, Z. Liao, S. Yang, and Y. Wang, "Image matching based on orientation–magnitude histograms and global consistency," *Pattern Recognit.*, vol. 45, no. 10, pp. 3825–3833, Oct. 2012.
[16] A. Ghaffari and E. Fatemizadeh, "Image registration based on low rank matrix: Rank-regularized SSD," *IEEE Trans. Med. Imag.*, vol. 37, no. 1, pp. 138–150, Jan. 2018.
[17] Y. Ye, J. Shan, L. Bruzzone, and L. Shen, "Robust registration of multimodal remote sensing images based on structural similarity," *IEEE Trans. Geosci. Remote Sens.*, vol. 55, no. 5, pp. 2941–2958, Mar. 2017.
[18] W. Ma, Y. Wu, Y. Zheng, Z. Wen, and L. Liu, "Remote sensing image registration based on multifeature and region division," *IEEE Geosci. Remote Sens. Lett.*, vol. 14, no. 10, pp. 1680–1684, Oct. 2017.
[19] H. Zhu, W. Ma, B. Hou, and L. Jiao, "SAR image registration based on multifeature detection and arborescence network matching," *IEEE Geosci. Remote Sens. Lett.*, vol. 13, no. 5, pp. 706–710, May 2016.
[20] S. Wang, H. You, and K. Fu, "BFSIFT: A novel method to find feature matches for SAR image registration," *IEEE Geosci. Remote Sens. Lett.*, vol. 9, no. 4, pp. 649–653, Jul. 2012.
[21] F. Dellinger, J. Delon, Y. Gousseau, J. Michel, and F. Tupin, "SAR-SIFT: A SIFT-like algorithm for SAR images," *IEEE Trans. Geosci. Remote Sens.*, vol. 53, no. 1, pp. 453–466, Jan. 2015.
[22] W. Ma *et al.*, "Remote sensing image registration with modified SIFT and enhanced feature matching," *IEEE Geosci. Remote Sens. Lett.*, vol. 14, no. 1, pp. 3–7, Jan. 2017.
[23] J. Fan, Y. Wu, F. Wang, P. Zhang, and M. Li, "New point matching algorithm using sparse representation of image patch feature for SAR image registration," *IEEE Trans. Geosci. Remote Sens.*, vol. 55, no. 3, pp. 1498–1510, Mar. 2017.
[24] M. A. Fischler and R. Bolles, "Random sample consensus: A paradigm for model fitting with applications to image analysis and automated cartography," *Commun. ACM*, vol. 24, no. 6, pp. 381–395, Jun. 1981.
[25] Y. Wu, W. Ma, M. Gong, L. Su, and L. Jiao, "A novel point-matching algorithm based on fast sample consensus for image registration," *IEEE Geosci. Remote Sens. Lett.*, vol. 12, no. 1, pp. 43–47, Jan. 2015.
[26] M. Chen, A. Habib, H. He, Q. Zhu, and W. Zhang, "Robust feature matching method for SAR and optical images by using Gaussian-gamma-shaped bi-windows-based descriptor and geometric constraint," *Remote Sens.*, vol. 9, p. 882, Aug. 2017.
[27] J. Li, Q. Hu, and M. Ai. (2018). "RIFT: Multi-modal image matching based on radiation-invariant feature transform." [Online]. Available: https://arxiv.org/abs/1804.09493
[28] J. Ma, J. Jiang, H. Zhou, J. Zhao, and X. Guo, "Guided locality preserving feature matching for remote sensing image registration," *IEEE Trans. Geosci. Remote Sens.*, vol. 56, no. 8, pp. 4435–4447, Aug. 2018.
[29] G. Mabuza-Hocquet and F. Nelwamondo, "Fusion of phase congruency and Harris algorithm for extraction of iris corner points," in *Proc. ICAI*, 2015, pp. 315–320.
[30] P. Kovesi, "Phase congruency detects corners and edges," in *Proc. DICTA*, Sydney, NSW, Australia, 2003, pp. 309–318.
[31] B. Fan, F. Wu, and Z. Hu, "Towards reliable matching of images containing repetitive patterns," *Pattern Recognit. Lett.*, vol. 32, no. 14, pp. 1851–1859, Oct. 2011.
[32] M. Hasan, X. Jia, A. Robles-Kelly, J. Zhou, and M. R. Pickering, "Multi-spectral remote sensing image registration via spatial relationship analysis on sift keypoints," in *Proc. Int. Geosci. Remote Sens. Symp.*, Jul. 2010, pp. 1011–1014.
[33] J. Debayle and B. Presles, "Rigid image registration by general adaptive neighborhood matching," *Pattern Recognit.*, vol. 55, pp. 45–57, Jul. 2016.
[34] B. Wang, J. Zhang, L. Lu, G. Huang, and Z. Zhao, "A uniform SIFT-like algorithm for SAR image registration," *IEEE Geosci. Remote Sens. Lett.*, vol. 12, no. 7, pp. 1426–1430, Jul. 2015.
[35] X. Yuan and P. Shi, "Iris feature extraction using 2D phase congruency," in *Proc. ICITA*, Sydney, NSW, Australia, 2005, pp. 437–441.
[36] L. Wang, C. Zhang, Z. Liu, B. Sun, and H. Tian, "Image feature detection based on phase congruency by monogenic filters," in *Proc. CCDC*, Changsha, China, 2014, pp. 2033–2038.
[37] M. C. Morrone, J. Ross, D. C. Burr, and R. Owens, "Mach bands are phase dependent," *Nature*, vol. 324, no. 6049, pp. 250–253, Nov. 1986.
[38] R. Dalvi and R. Abugharbieh, "Fast feature based multi slice to volume registration using phase congruency," in *Proc. EMBC*, Vancouver, BC, Canada, 2008, pp. 5390–5393.
[39] J. Ma, H. Zhou, J. Zhao, Y. Gao, J. Jiang, and J. Tian, "Robust feature matching for remote sensing image registration via locally linear transforming," *IEEE Trans. Geosci. Remote Sens.*, vol. 53, no. 12, pp. 6469–6481, Dec. 2015.
[40] P. Du, X. Shi, N. Wang, and R. Deng, "Iris recognition based on principal phase congruency," in *Proc. CCDC*, Taiyuan, China, 2012, pp. 1159–1162.
[41] P. Coupé, J. V. Manjón, V. Fonov, J. Pruessner, M. Robles, and D. L. Collins, "Patch-based segmentation using expert priors: Application to hippocampus and ventricle segmentation," *NeuroImage*, vol. 54, no. 2, pp. 940–954, Jan. 2011.
[42] D. G. Lowe, "Distinctive image features from scale-invariant keypoints," *Int. J. Comput. Vis.*, vol. 60, no. 2, pp. 91–110, Nov. 2004.
[43] H. Bay, A. Ess, T. Tuytelaars, and L. Van Gool, "Speeded-up robust features (SURF)," *Comput. Vis. Image Understand.*, vol. 110, no. 3, pp. 346–359, Jun. 2008.
[44] B. Li and H. Ye, "RSCJ: Robust sample consensus judging algorithm for remote sensing image registration," *IEEE Geosci. Remote Sens. Lett.*, vol. 9, no. 4, pp. 574–578, Jul. 2012.

WENPING MA (M'07) received the B.S. degree in computer science and technology and the Ph.D. degree in pattern recognition and intelligent systems from Xidian University, Xi'an, China, in 2003 and 2008, respectively. Since 2006, she has been with the Key Laboratory of Intelligent Perception and Image Understanding, Ministry of Education, Xidian University, where she is currently an Associate Professor. She has published more than 30 SCI papers in international academic journals, including the IEEE TRANSACTIONS ON EVOLUTIONARY COMPUTATION, IEEE TRANSACTIONS ON IMAGE PROCESSING, *Information Sciences*, *Pattern Recognition*, *Applied Soft Computing*, *Knowledge-Based Systems*, *Physica A-Statistical Mechanics and its Applications*, and IEEE GEOSCIENCE AND REMOTE SENSING LETTERS. Her research interests include natural computing and intelligent image processing.

Dr. Ma is a member of the Chinese Institute of Electronics and the China Computer Federation.

YUE WU received the B.S. and Ph.D. degrees from Xidian University, Xi'an, China, in 2011 and 2016, respectively. Since 2016, he has been a Teacher with Xidian University. He has published over 30 refereed journal and conference papers. He was invited to work as the Registration Chair of BIC-TA 2016. His research interests include computer vision and computational intelligence.

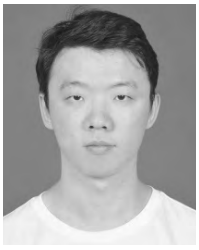

SHAODI LIU was born in Gongyi, Henan, China, in 1995. He received the B.S. degree in intelligent science and technology from Xidian University, Xi'an, China, in 2017, where he is currently pursuing the M.S. degree. His research interests include image registration and evolutionary computation.

QINGXIU SU received the B.S. degree from the Jiangsu University of Science and Technology, Zhenjiang, China, in 2017. She is currently pursuing the M.S. degree with Xidian University. Her research interests include image registration and feature matching.

YONG ZHONG received the B.S. degree in control technology and instruments and the M.S. degree in circuits and systems from Xidian University, Xi'an, China, in 2015 and 2018, respectively. His research interests include remote sensing image registration and computational intelligence.